

## **Investigation of the Gas Dynamics in an Upflow OMVPE Reactor by Raman Spectroscopy**

Chinho Park\* and Timothy J. Anderson\*\*

\*Yeungnam University, School of Chemical Engineering and Technology, Kyongsan 712-749, Korea

\*\*University of Florida, Chemical Engineering Department, Gainesville, FL 32611, U.S.A.

### **ABSTRACT**

The gas dynamics in a stagnation point upflow OMVPE reactor were studied by Raman spectroscopy. The gas temperature was measured as a function of inlet gas velocity and aspect ratio for both H<sub>2</sub> and N<sub>2</sub> carrier gases. The centerline temperature gradient was larger at higher inlet velocities and with the use of N<sub>2</sub>, and only weakly dependent on the aspect ratio. A tracer molecule, CH<sub>4</sub>, was used to investigate the steady state behavior of reactants in the reactor, and the use of a sweeping flow was found to be a suitable method for preventing wall deposition. The transient switching response of the gas manifold was also investigated. Under certain conditions (low velocities, unmatched flows) recirculation flows were apparent. Numerical calculations of the reactor gas dynamics gave reasonable agreement with the experimental results when detailed thermal boundary conditions were included.

## INTRODUCTION

Organo-Metallic Vapor Phase Epitaxy (OMVPE) has proven to be a versatile technique to grow thin films of a variety of materials (1). The uniformity of the deposited layers and the abruptness of heterojunctions are strongly influenced by the gas dynamics in the reactor. It is desirable to establish a uniform flow field in the reactor that is free of laminar vortices to minimize the gas residence time and the reactant switching time. Gas phase isotherms parallel to the substrate are also desirable to achieve uniform growth, and isotherms confined to the vicinity of the substrate help to minimize parasitic gas phase reactions and reject particles. A large temperature gradient normal to the substrate surface can, however, produce recirculating flow patterns in the reactor causing growth rate variations, increased impurity incorporation, and graded heterojunctions (2). Gas switching mechanism can also affect the layer abruptness due to the dead space formed in the gas switching manifold and the long transient response caused by pressure imbalance between the vent and run sides (3). Eddy currents formed at the gas inlets could serve as memory cells of reactant gases (4). Thus it is very important to understand the gas dynamics in the reactor when a growth system is designed and built.

This study reports measurement of the gas dynamics in a stagnation point upflow OMVPE reactor using Raman spectroscopy. Temperature profile in the reactor was measured by the rotational Raman scattering from the carrier gas ( $N_2$  or  $H_2$ ) molecules. Steady state behavior of the reactants and their transient response were investigated by the vibrational Raman scattering from the tracer molecule ( $CH_4$ ) in the gas stream.

## EXPERIMENTAL

The experimental apparatus consisted of a stagnation point upflow OMVPE reactor system interfaced with a Ramanor U-1000 Raman spectrometer. A schematic diagram of the experimental set up is shown in Figure 1. An upflow configuration was adopted to reduce the buoyancy driven flow recirculation phenomena frequently encountered in commercial reactors using horizontal or vertical downflow geometry. Two separate gas flow streams were provided to the reactor. The center flow served to supply the tracer species ( $CH_4$ ) diluted in the carrier gas ( $N_2$  or  $H_2$ ), while a sweeping flow containing only the carrier gas surrounded the center flow. The reactor was mounted on a micrometer controlled x-y-z stage located in the macro-chamber of the Raman spectrometer to permit spatially resolved measurement of the gas temperature and the concentration of a tracer species by analysis of the Raman scattered light. The gas manifold had a vent/run capability by 3-way valves for reactant switching, and it also contained the make-up carrier gas supplies to minimize flow disturbances during the switching operation.

The 488 nm light from an Ar-ion laser was used as the excitation source at a laser power of 1 W. A photomultiplier tube (PMT) was used as a detector, and photon counting electronics were employed. The spatial resolutions of about 30  $\mu m$  in the y and z direction and about 3000  $\mu m$  in the x direction were easily obtained. A more detailed description of the experimental system is presented elsewhere (5,6).

## RESULTS AND DISCUSSION

The gas temperature was measured by pure rotational Raman scattering from the carrier gas molecules,  $N_2$  or  $H_2$ , as a function of the inlet gas velocity and the aspect ratio (AR : ratio of

the distance between the susceptor and the center inlet tube to the center tube diameter). The technique is well established with theoretical backgrounds (7). The centerline temperature gradient was greater with a higher inlet velocity and with the use of  $N_2$ , and only weakly dependent on the aspect ratio. As an example, the effect of changing the inlet gas velocity on the measured axial temperature profile along the center line for a susceptor temperature ( $T_{set}$ ) of 650 °C is shown in Figure 2 along with the results of a 2-dimensional simulation using axisymmetric model. As expected, increasing the inlet velocity produced a steeper gradient primarily because of the reduced residence time. At low inlet velocities, the inlet gas temperature is observed to be greater than the ambient temperature due to radiative heat transfer to the inlet manifold exceeding convective or conductive losses. The extrapolated surface temperature of the susceptor is seen to be almost 200 °C less than the set point temperature measured by the control thermocouple, apparently because of thermal contact resistance between the heater and the susceptor. The accuracy of the measured temperature depended on the signal to noise ratio which decreases with increasing temperature, and the uncertainty of the temperature was less than  $\pm 20$  °C for most cases of this study. The repeatability of the temperature measurement was found to be excellent. The calculated temperature profiles gave reasonably good agreement with the experimental results when detailed thermal boundary conditions were included (6).

The dispersion characteristics and reactant switching response of the reactor were studied by vibrational Raman scattering from the tracer species,  $CH_4$ , introduced in the center inlet carrier gas stream. A sweeping flow of pure carrier gas surrounded the center inlet gas stream with the tracer species. The relative  $CH_4$  concentration profile parallel to the susceptor at various axial positions is shown in Figure 3 for a matched velocity of 2.4 cm/s (both center and sweeping flows) with the  $N_2$  carrier gas. The  $y$  position at 0 stands for the centerline of the reactor, and  $y = 38.1$  mm is at the reactor wall. The dashed lines in the middle of the figure represent the  $y$  positions of the inside edge and the outside edge of the center tube, respectively. The axial positions ( $z$ ) were measured from the center flow inlet. As shown in this figure, the dispersion was negligible. Increasing the susceptor temperature to  $T_{set} = 650$  °C did not introduce any new flow behavior other than those already observed in the room temperature experiments with the matched velocity of 2.4 cm/s. The center flow was very well confined in the center region with matched velocities. This is encouraging because one can expect that in actual epitaxial growth runs or in the kinetic experiments, the reacting species are confined in the center flow region, thus the wall deposition can be completely removed. Well-known memory effects (8) could also be prevented. The heavier mass (smaller diffusivity) of actual reactants (e.g.,  $TMIn$ ,  $PH_3$ , etc.) compared to that of  $CH_4$  further favors the situation. In fact, no depositions were observed at the reactor wall, when  $TMIn$  was introduced into the center flow, although depositions were observed on the sides of the furnace body. When the sweeping velocity was lowered to 0.6 cm/s (unmatched velocities), however, the dispersion was significant as appeared in Figure 4. Evidence of the establishment of recirculation flows was observed when the sweeping flow velocity did not match the center inlet velocity.

The switching response of the gas manifold was also characterized. As an example, Figure 5 shows the response of the reactor to a 20 second pulse of carrier gas containing the tracer species for three different matched inlet velocities. These data are consistent with the expected velocity dependence of the time lag due to dead volume and axial dispersion. A second  $CH_4$  spike that is apparent in the data for the lowest velocity studied (0.75 cm/s) is consistent with the presence of recirculation flows. The effect of unmatched flow velocities between the center and the sweeping flow was also studied, and the results are shown in Figure 6. A second shoulder spike was more clearly observed when the sweeping flow velocity was reduced to 0.75 cm/s from the matched velocity of 3.0 cm/s, which indicated that a recirculating flow was

developed in the reactor. This result is consistent with an observation in a steady flow conditions (Figure 4).

### CONCLUSIONS

Raman spectroscopy has been successfully applied to the investigation of the gas dynamics in a stagnation point upflow OMVPE reactor. The technique provides a spacially resolved measurement of the gas temperature and the concentration with high accuracy. The temperature profile study indicated that a larger temperature gradient normal to the susceptor surface could be achieved with a higher inlet flow velocity and with the use of a N<sub>2</sub> carrier gas. The gas phase dispersion of the reactants in the reactor and the transient switching response of the gas manifold were simulated by a CH<sub>4</sub> tracer experiment. It was found that the sweeping flow can be used as a suitable method for preventing wall deposition when the matched flow velocities are established between the center and the sweeping flows. Numerical calculations of the reactor gas dynamics using 2-dimensional axisymmetric model provided reasonably good agreement with the experimental results when detailed thermal boundary conditions were included.

### ACKNOWLEDGEMENTS

Authors would like to express special thanks to Mr. P. Axson for his support in the set-up of the experimental system. This work is supported in part by KÖSEF Grant #96-0300-14-01-3.

### REFERENCES

1. G.B. Stringfellow, in: *Organometallic Vapor-Phase Epitaxy: Theory and Practice*, Academic Press, San Diego, CA (1989).
2. K.F. Jensen, *J. Crystal Growth* **98** (1989) 148.
3. F. Agahi, C.R. Lutz and K.M. Lau, *J. Crystal Growth* **139** (1994) 344.
4. Y. Monteil, R. Favre, A. Bekkaoui, P. Raffin, J. Bouix, J. Marcillat and P. Dutto, *J. Crystal Growth* **93** (1988) 270.
5. Z.S. Huang, C. Park and T.J. Anderson, *J. Organomet. Chem.* **449** (1993) 77.
6. C. Park, A. Zhao and T.J. Anderson, submitted to *J. Crystal Growth* (1997).
7. H.W. Schrötter and H.W. Klöckner, in: *Raman Spectroscopy of Gases and Liquid*, Ed. A. Weber, Springer-Verlag, Berlin, Germany (1979) p.123.
8. Y. Ohba and A. Hatano, *J. Crystal Growth* **145** (1994) 214.

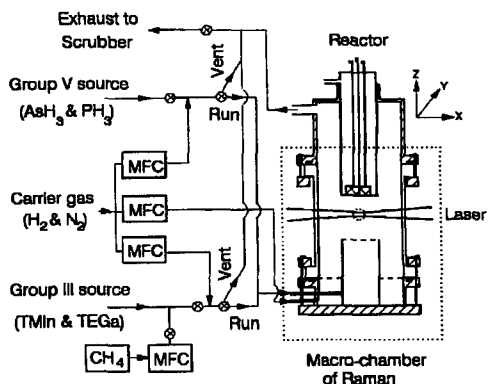


Figure 1. A schematic description of the experimental system.

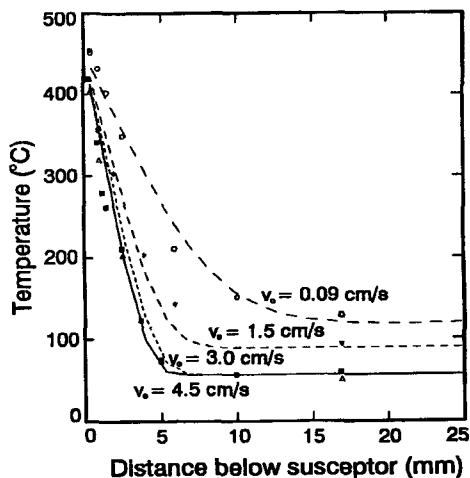


Figure 2. The effect of varying the gas inlet velocity on the axial centerline temperature profile in the reactor for  $N_2$  carrier gas. Calculated results (solid and dashed lines) are shown with the experimental data.  $AR = 1$ ,  $T_{set} = 650 \text{ }^\circ\text{C}$ .

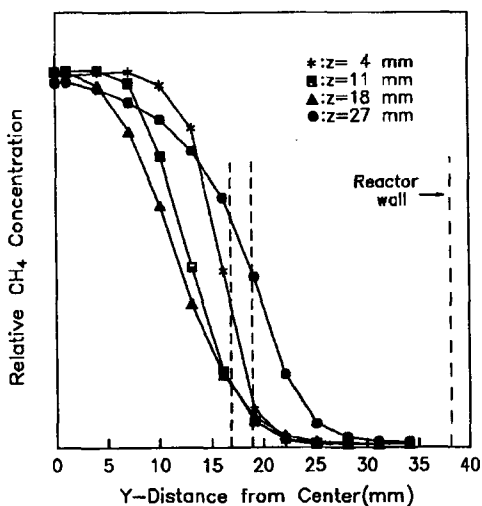


Figure 3. The relative  $CH_4$  concentration profiles along the y-axis: matched inlet flow velocities;  $N_2$  carrier gas;  $T_{set} = 25 \text{ }^\circ\text{C}$ ;  $AR = 0.9$ ;  $v_c = 2.4 \text{ cm/s}$ ;  $v_s = 2.4 \text{ cm/s}$ .

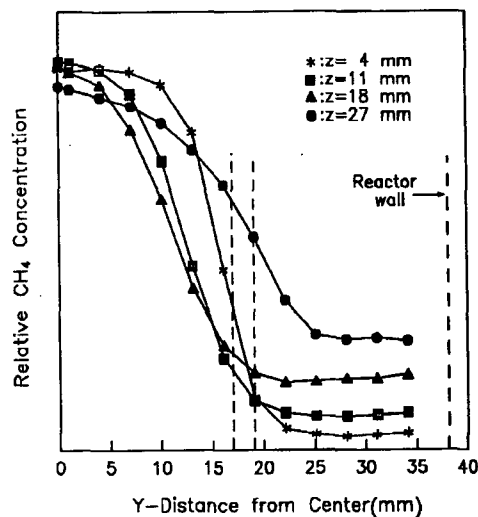


Figure 4. The relative  $CH_4$  concentration profiles along the y-axis: unmatched inlet flow velocities;  $N_2$  carrier gas;  $T_{set} = 25 \text{ }^\circ\text{C}$ ;  $AR = 0.9$ ;  $v_c = 2.4 \text{ cm/s}$ ;  $v_s = 0.6 \text{ cm/s}$ .

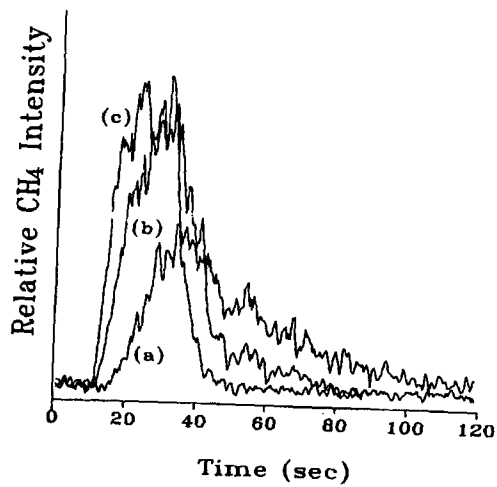


Figure 5. Time response of the reactor for matched  $H_2$  carrier velocities:  $T_{set} = 25\text{ }^\circ\text{C}$ ;  $AR = 1$ ; (a)  $v_c = 0.75\text{ cm/s}$ ,  $v_s = 0.75\text{ cm/s}$ ; (b)  $v_c = 1.5\text{ cm/s}$ ,  $v_s = 1.5\text{ cm/s}$ ; (c)  $v_c = 3.0\text{ cm/s}$ ,  $v_s = 3.0\text{ cm/s}$ . Probe position is at 12 mm below the susceptor in the axial centerline.

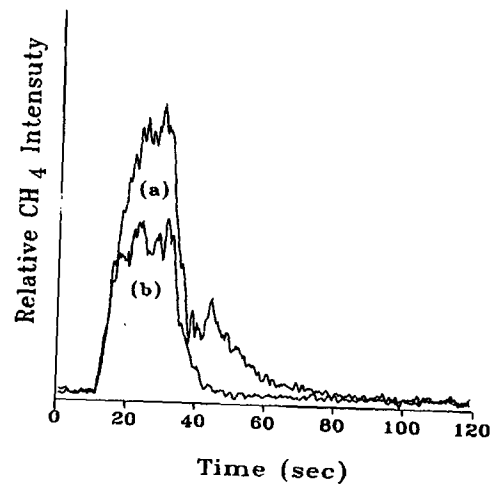


Figure 6. Time response of the reactor for matched and unmatched  $H_2$  carrier velocities:  $T_{set} = 25\text{ }^\circ\text{C}$ ;  $AR = 1$ ; (a)  $v_c = 3.0\text{ cm/s}$ ,  $v_s = 3.0\text{ cm/s}$ ; (b)  $v_c = 3.0\text{ cm/s}$ ,  $v_s = 0.75\text{ cm/s}$ . Probe position is 12 mm below the susceptor in the axial centerline.